HHS Public Access
Author manuscript
Cancer Res. Author manuscript; available in PMC 2018 June 01.

GAD1 Upregulation Programs Aggressive Features of Cancer Cell Metabolism in the Brain Metastatic Microenvironment

Patricia M. Schnepp[1,2], **Dennis D. Lee**[1], **Ian H. Guldner**[1,2], **Treasa K. O'Tighearnaigh**[1], **Erin N. Howe**[1,2], **Bhavana Palakurthi**[1], **Kaitlyn E. Eckert**[3], **Tiffany A. Toni**[3], **Brandon L. Ashfeld**[2,3], and **Siyuan Zhang**[1,2,4,*]

[1]Department of Biological Sciences, College of Science, University of Notre Dame, Notre Dame, IN 46556, USA

[2]Mike and Josie Harper Cancer Research Institute, University of Notre Dame, 1234 N. Notre Dame Avenue, South Bend, IN 46617, USA

[3]Department of Chemistry and Biochemistry, University of Notre Dame, Notre Dame, IN 46556, USA

[4]Indiana University Melvin & Bren Simon Cancer Center, 535 Barnhill Drive, Indianapolis, IN 46202, USA

Abstract

The impact of altered amino acid metabolism on cancer progression is not fully understood. We hypothesized that a metabolic transcriptome shift during metastatic evolution is crucial for brain metastasis. Here we report a powerful impact in this setting caused by epigenetic upregulation of glutamate decarboxylase 1 (GAD1), a regulator of the GABA neurotransmitter metabolic pathway. In cell-based culture and brain metastasis models, we found that downegulation of the DNA methyltransferase DNMT1 induced by the brain microenvironment-derived clusterin resulted in decreased GAD1 promoter methylation and subsequent upregulation of GAD1 expression in brain metastatic tumor cells. In a system to dynamically visualize cellular metabolic responses mediated by GAD1, we monitored the cytosolic NADH:NAD$^+$ equilibrium in tumor cells. Reducing GAD1 in metastatic cells by primary glia cell co-culture abolished the capacity of metastatic cells to utilize extracellular glutamine, leading to cytosolic accumulation of NADH and increased oxidative status. Similarly, genetic or pharmacological disruption of the GABA metabolic pathway decreased the incidence of brain metastasis in vivo. Taken together, our results show how epigenetic changes in GAD1 expression alter local glutamate metabolism in the brain metastatic microenvironment, contributing to a metabolic adaption that facilitates metastasis outgrowth in that setting.

Keywords

Brain metastasis; epigenetic regulation; cancer metabolism; metastatic adaptation; metastatic microenvironment; GABA pathway; drug repurposing

*Correspondence to: Siyuan Zhang, M.D., Ph.D., Department of Biological Sciences, University of Notre Dame, A130 Harper Hall, Notre Dame, IN 46556. szhang8@nd.edu; Telephone: 713-792-3636; Fax: 713-792-4454.

Introduction

Altered cancer cell metabolism has been recognized as one of the important hallmarks of cancer(1,2). The dynamic metabolic balance between metabolic stress and the high demand for macromolecules for enhanced proliferation in the tumor cell is highly tissue context-dependent(1). The process of metastasis represents an extreme case of context-dependent metabolic adaptation(3). Recently, experimental evidence began to shed light on the critical role of the metabolic interactions between tumor cells and the metastatic tumor microenvironment in facilitating metastatic success. Direct lipid transfer from peritoneal adipocytes to metastatic ovarian cancer cells promotes omental metastasis(4). Colon cancer cell-derived creatine kinase promotes the synthesis of phosphocreatine, which is transported and catabolized by metastatic tumor cells to generate ATP(5). Additionally, an *in vitro* proteomics analysis of brain-seeking sub-clones of a breast cancer cell line showed an increase in proteins that regulates β-oxidation of fatty acid synthesis, glycolysis and TCA-cycle activity compared to the parental lines, implying a role for the brain microenvironment in reshaping metastatic tumor cell metabolism(6). Yet, the mechanisms of how metastatic tumor cells acquire a new metabolic balance when surrounded by a highly metabolically unique brain microenvironment are still poorly understood.

In normal physiological conditions, the brain microenvironment displays a unique metabolic cooperation among diverse cells types. Global brain tissue metabolism is compartmentalized between different cellular subtypes(7). This compartmentalized metabolic phenotype requires dynamic cross-talk between various cell types to establish a cohesive metabolic signaling network(8,9). Highly active neurons require an uninterrupted supply of metabolites from the astrocyte-neuron metabolic shuttle – lactate, glutamate, glutamine, malate and α-ketoglutarate(10–13). Interestingly, recent studies have revealed crosstalk between brain astrocytes and metastatic tumor cells that is reminiscent of astrocyte-neuron interactions, including down-regulation of the tumor suppressor PTEN through uptake of glia-derived exosomes(14), and gap junctions mediated transfer of cGAMP to astrocytes(15). Intriguingly, clinical brain metastases display an increased neuronal-like gene signature compared with primary tumor counterparts, suggesting metastatic tumor cells engage an extensive brain-like transcriptome adaptation(16,17). However, it is still unknown whether the neuronal-like properties obtained by the metastatic tumor cell facilitate a neuronal-like metabolic adaption to efficiently utilize the metabolites in the extracellular compartment of the brain.

In this study, we identified the brain microenvironment-dependent up-regulation of glutamate decarboxylase 1 (GAD1) in metastatic cancer cells, which facilitates glutamine metabolism and intracellular γ-aminobutyric acid (GABA) production. Mechanistically, we elucidated that epigenetic regulation induced by the brain microenvironment-derived clusterin resulted in an up-regulation of GAD1 expression and functionally necessitated sustained brain metastatic outgrowth. Furthermore, our results revealed a novel therapeutic opportunity for brain metastasis patients. GAD1-GABA-dependent metastasis outgrowth warrants an alternative therapeutic strategy by repurposing FDA approved blood-brain barrier (BBB) permeable GABA targeting agent. Here, we demonstrate that vigabatrin, a

clinically approved anti-epileptic seizure drug targeting the catabolism of GABA downstream of GAD1, showed a promising therapeutic efficacy in treating brain metastasis *in vivo*. In summary, our study provides mechanistic insight into brain microenvironment-induced epigenetic regulation of GAD1. Our pre-clinical evidence of repurposing anti-seizure agents as novel anti-brain metastatic treatment opens new translational avenues, which could yield more effective clinical therapeutics for patients who are desperate for a cure.

Materials and Methods

Reagents and Cell Culture

A375SM and MDA-MB-231 cell lines were purchased from ATCC in the past three years and cultured less than six months before replenishment. Cells were authenticated by short tanden repeat less than six months prior to publication. All cell lines were tested mycoplasma negative. Human cell lines were further authenticated using STR Profiling by Genetica DNA Laboratories (Burlington, NC). Primary glia cells were isolated from brain tissue of new born C57B6 mouse pups (1 to 3 days old) as described(18). Cancer associated fibroblast (CAF) cell line was a gift from Dr. Zachary Schafer at the University of Notre Dame. Lentiviral-based expression vectors pcDNA3/Myc-DNMT1 (36939), pcDNA3.1-Peredox-mCherry (32383) and packaging vectors were purchased from Addgene. Lentiviral-based TRIPZ short hairpin RNA (shRNA) and SMARTpool:ON-TARGETplus siRNA were purchased from GE Healthcare. MISSION esiRNA and GABRA1 (HPA055746) antibody were purchased from Sigma-Aldrich. DNMT3A (ab4897) and p-AMPK (ab131357) antibodies were purchased from Abcam. DNMT1 (5032) and DNMT3B (67259) antibodies were purchased from Cell Signaling Technology. For co-culture experiments, tumor cells were mixed in a 1:5 ratio with either freshly isolated primary glia or CAF cells in six-well plates. For the transwell co-culture experiments, tumor cells were seeded in the bottom wells and primary glia or CAF cells were seeded on the upper insert and maintained for two days. For conditioned media and co-culture experiments, reduced media (1 g/L glucose, 2 mM L-glutamine, 10% of fetal bovine serum, 1% penicillin/streptomycin) was used. Conditioned media were collected five days after seeding of either glia or CAF cells. Conditioned media were mixed with fresh media as designated and used as culture media for tumor cell proliferation assay. Cytokine array analysis was conducted by RayBiotech (Quantibody Mouse Cytokine Array 4000). Human clusterin protein (2937-HS-050) was purchased from R&D systems. Clusterin siRNA (mouse, sc-43689) was purchased from Santa Cruz Biotechnology.

Bioinformatics and Gene Set Enrichment Analysis (GSEA)

Publically available GSE19184 dataset(19) was analyzed for transcriptome changes of tumor cell at the different tissue microenvironments. In brief, we performed differential gene expression analysis using the Comparative Selection Marker Module interface to compare the transcriptome profile of brain metastases to respective primary tumor. Four tumor types are analyzed: MDA-MB-231Br3 for mammary tumor, PC14Br4 for prostate tumor, A375SM for melanoma, KM12M for cecum cancer. A q-value of less than 0.05 was considered statistically significant. To identify metabolism related genes, we performed

GSEA analysis(20) using GenePattern interface (http://www.broadinstitute.org/gsea/) (21). Metabolism specific custom gene sets were assembled from the MSigDB v4.0 database(20), specifically from c2 and c5 sub-databases. GSEA enrichment results were compared across all four cell lines to identify shared enriched gene sets. The differently expressed metabolic genes were depicted by Java Treeview. Network analysis were conducted through the web-based bioinformatics package NetworkAnalyst (http://www.networkanalyst.ca) based on recommended protocol(22,23).

Quantitative Real-Time PCR (qRT-PCR)

Total RNA was isolated using TRIzol® reagent (Life Technologies) and then reverse-transcribed using Verso cDNA Synthesis Kit (Thermo Fisher Scientific). SYBR-based qRT-PCR was performed using pre-designed primers. For quantification of gene expression, real-time PCR was conducted using iTaq™ Universal SYBR® Green Supermix (Bio-rad) on a Mastercycler® ep *realplex* real-time PCR machine (Eppendorf). The relative expression of mRNAs was quantified by $2^{-\Delta Ct}$ with logarithm transformation.

Proliferation Assay

Tumor cells were seeded in 1:5 ratio of tumor to stromal cell and cultured for 48 hours in reduced media. Five random non-overlapping regions were imaged using a Zeiss Axio confocal microscope. Three wells were manually counted for each condition.

DNA Extraction and Methylation Analysis

Genomic DNA was extracted from 25 mg of brain tissue containing human metastatic tumors or 100,000 tumor cells with the DNeasy blood and tissue kit (Qiagen). DNA (1 μg) was modified with sodium bisulfite (EpiTect kit, Qiagen). For methylation specific PCR, 100 ng of converted DNA was amplified with the EpiTect MSP kit (Qiagen) using specific methylated or unmethylated primers designed with MethPrimer(24) and following the cycling conditions indicated by the EpiTect MSP kit. For bisulfite sequencing, GAD1 promoter region (CpG island 122) was amplified and gel purified. Sanger DNA sequencing was performed on purified PCR amplicon.

Biosensors and Time-lapse Imaging

Tumor cells were transiently transfected Peredox(25) and co-cultured with either CAF or glia cells in reduced media conditions for 48 hours. For time-lapse imaging, cells were incubated in an environment chamber (5% CO_2 and 37°C) with a consistent media flow (0.5 ml/min). Glutamine was supplemented for a final concentration of 2 mM. Cells were maintained in initial reduced media condition for 10 minutes prior to image acquisition. Time-lapse imaging was performed on a Nikon A1-R confocal microscope (ex:488 nm em: 561 nm). ImageJ and custom MatLab codes were used to subtracted background, determined fluorescent intensity and generated pixel-by-pixel green-to-red ratio image for each time point. Fluorescence baseline value of each cell at the initial time point was defined as relative level 1.0.

In vivo animal experiments

All animal experiments and terminal endpoints were carried out in accordance with approved protocols by Notre Dame Institutional Animal Care and Use Committee. Primary mammary fat pad (MFP) tumors were established by injection of 5×10^6 tumor cells orthotopically into the MFP of 12 week old Rag1$^{-/-}$ mice. Brain metastatic tumors were established by either intracarotid injection of tumor cells (250,000 cells in 0.1 ml of serum free media) or intracranial injection (50,000 cells in 2 μl of serum free media). The endpoints of *in vivo* experiments are based on the presence of clinical signs of brain metastasis, including but not limited to, primary central nervous system disturbances, weight loss, and behavior abnormalities. Animals are culled after showing the above signs or 3 week after surgery. Eight haematoxylin and eosin (H&E)-stained sagittal sections through the left hemisphere of the brain were analyzed for the presence of metastatic lesions. Brain metastases incidence was quantified by identification of tumors from fluorescent images of total brain (A375SM) or by identification of tumors from H&E stained sections (MDA-MB-231).

Immunohistochemistry (IHC) and Immunofluorescence (IF) staining

Standard immunohistochemistry was performed as described previously(14). Immunofluorescence was performed following the standard protocol (Cell Signaling Inc.). ImageJ was used for quantification of pixel-by-pixel intensity of staining.

Statistical Analysis

For quantitative data with normal distribution, the Student *t* test was used for comparing two groups. All *p* values are two-tailed. A difference with $p < 0.05$ (two-sided) was considered statistically significant.

Results

Brain Metastatic Microenvironment Induces a Global Metabolic Transcriptome Shift

To examine the global influence of the brain metastatic microenvironment on cancer cell metabolism *in vivo*, we performed bioinformatics analysis focusing on curated metabolism related genes using a publically available cDNA microarray dataset (GSE19184), containing gene expression data generated from either primary xenograft tumors or brain metastases counterparts. This dataset represents major tumor types that metastasize to the brain, including lung (KM12M), colon (PC14Br4), melanoma (A375SM) and breast (MDA-MB-231Br3). Surprisingly, we observed a global down-regulation of the majority of metabolism related genes in brain metastatic tissues compared with respective primary tumors, regardless of their distinct primary tumor-of-origin (Fig 1A). In contrast, only a small set of metabolism related genes were up-regulated in brain metastases (Fig 1A, top right), suggesting that brain metastases engage a specific metabolic program that is vital for sustaining their energy needs. We performed GSEA to further determine the functional implications of the tumor metabolic shift. Interestingly, despite the majority of metabolism related gene sets were negatively enriched in the brain metastatic tumors, only one gene set (REACTOME: GABA synthesis, release, reuptake, and degradation) was significantly

enriched in the brain metastatic tumors in all four cell lines (Fig 1B-D, Supplementary Fig S1 and Supplementary Table 1). γ-aminobutyric acid (GABA) is an inhibitory neurotransmitter primarily found in GABAergic neurons(26). In line with a recent clinical finding demonstrating GABA receptor up-regulation in human HER2+ breast cancer brain metastases(16), enrichment of GABA signaling in brain metastatic tumor cells suggests that the metastatic tumor cells might adapt and shift to more neuronal-like signaling to thrive in the brain microenvironment. To mimic the brain microenvironment, we co-cultured MDA-MB-231Br cells with primary brain glia cells and observed an increase in one GABA receptor isoform, GABRA1, compared to tumor cells alone (Supplementary Fig S2A). Examining the "REACTOME: GABA synthesis, release, reuptake, and degradation" gene set further revealed glutamate decarboxylase 1 (GAD1) as among the only three significantly up-regulated genes in brain metastases (Fig 2A). GAD1 catalyzes the production of GABA from L-glutamic acid and is primarily found in the cytosol in order to provide an intracellular source of GABA for cell metabolism(27). As other cellular processes to catabolize glutamine (and glutamate) were down-regulated (Supplementary Fig S2B-C and Supplementary Table 2) in brain metastatic tumor cells, we reasoned that the GAD1-mediated GABA pathway could be the primary method for utilizing glutamine as an energy source in metastatic tumor cells.

To validate the observed increase of GAD1 in brain metastases from our bioinformatics analysis, we injected MDA-MB-231 parental cells (MDA-MB-231 here after), a non-brain-seeking triple-negative breast cancer cell line, into either the brain or mammary fat pad to model brain metastases and primary breast cancer. Using human specific qRT-PCR primers, we detected a significant increase of GAD1 mRNA expression in the brain metastatic tumor compared to the primary tumors (Fig 2B, $p < 0.01$). To model the different tissue microenvironments *in vitro*, we co-cultured tumor cells with either Cav1$^{-/-}$ fibroblast (cancer associated fibroblast, CAF) cells or primary glia cells to model the primary cancer microenvironment or brain metastatic microenvironment respectively(14,28). Compared with CAF co-culture, co-culture with primary glia cells led to a significant increase of GAD1 mRNA expression in both MDA-MD-231 cells and A375SM cells (Fig 2C, $p < 0.01$), which was associated with increased cell proliferation of tumor cells (Fig 2D, left, $p < 0.001$). Importantly, the proliferative advantage imposed by glia co-culture was completely abolished by inducible knockdown of GAD1 in tumor cells (Fig 2D, right, $p < 0.0005$ and Supplementary Fig 3, $p < 0.0001$). Together, this data demonstrates that the brain metastatic microenvironment alters the cancer cell metabolic transcriptome and induces up-regulation of GAD1 mRNA expression, thereby facilitating tumor cell proliferation.

Brain Microenvironment-induced Down-Regulation of DNMT1 Reactivates GAD1 Expression

Epigenetic regulation has been implicated in regulation of GAD1 gene expression under certain pathological conditions, such as schizophrenia(29). We examined the ENCODE data track of the GAD1 genomic locus(30), and found that CpG islands located on the GAD1 promoter are heavily methylated in differentiated cancer cell lines (K562, HeLa and HepG2) while de-methylated in human embryonic stem cells (hESC) (Fig 3A). This suggests a possible methylation-dependent regulation of GAD1 mRNA transcription(31). We first

performed methylation-specific PCR (MSP) using human specific primers to multiple CpG sites along the GAD1 promoter (Supplementary Fig S4). Co-culture with glia cells decreased GAD1 promoter methylation compared with co-culture with CAFs (Fig 3B). Bisulfate sequencing of CpG Island 122 located in the GAD1 promoter further validated a decreased GAD1 promoter methylation under the glia cell co-culture (Fig 3C, p < 0.05). Consistently, *in vivo* brain metastases exhibited a similar decrease in GAD1 promoter methylation compared to paired primary tumors (Fig 3D).

As the primary enzyme regulating the propagation of DNA methylation(32), DNA (cytosine-5)-methyltransferase 1 (DNMT1) has been shown to regulate GAD1 through DNA methylation in multiple physiological conditions(29). Interestingly, we observed a significant decrease of DNMT1 mRNA in brain metastatic tissue compared with paired primary tumors derived from A375SM and MDA-MB-231Br3 cells (q < 0.005 and q < 0.001 respectively) in our bioinformatics analysis of GSE19184 (Fig 3E). Moreover, we detected a significant reduction of DNMT1 mRNA expression using independent, paired tumor sets (brain vs. primary) (Fig 3F, p < 0.0001) and co-cultured with glia, but not CAF cells, led to a prominent decrease in DNMT1 mRNA expression in both MDA-MB-231 and A375 cells (Fig 4A, p < 0.005 and p <0.001 respectively). Consistently, DNMT1 protein expression was also decreased in glia co-culture (Supplementary Fig S5A), while there are no evident changes in DNMT3A and DNMT3B mRNA and protein (Supplementary Fig S5B-D). The above evidence suggests that the brain microenvironment induces de-methylation of the GAD1 promoter, possibly through down-regulation of DNMT1. To determine whether the altered DNMT1 expression in tumor cells induced by glia co-culture requires direct cell-to-cell contact, we cultured tumor cells using conditioned media from either glia or CAF cells. Culture with glia-conditioned media, but not CAF-conditioned media, reduced DNMT1 mRNA expression (Fig 4B, p < 0.05). Consistently, when we cultured tumor and stromal cells in a transwell system, we observe a similar decrease in DNMT1 expression (Supplementary Fig S5E, gray boxes, p < 0.005) and a corresponding increase in GAD1 expression (Supplementary Fig S5E, white boxes, p < 0.005), suggesting an unique glia secretory factors influence DNMT1 gene expression in tumor cells. Next, we conducted an unbiased cytokine screen to identify the glia secretory factor influencing the epigenetic regulation of GAD1 in tumor cells. We identified 74 differentially expressed cytokines between conditioned media from glia cells or CAF cells (Fig 4C, left, adjusted p < 0.1) with 44 cytokines enriched in glia conditioned media (Fig 4C, right, heatmap). We further performed Network analysis using online NetworkAnalyst tools. We constructed densely connected modules and nodes based on the number of first-degree interactions. Interestingly, NetworkAnalyst revealed the cytokine clusterin as the top-ranked key nodes (centrality degree=74, betweeness= 17320.89) (Fig 4D and Supplementary Table 3) and is highly expressed in the glia conditioned media (Fig 4E, left, p < 0.05). Clusterin is a glycoprotein increased in pathological conditions that has been implicated in cancer and cellular adaptive responses to extracellular stresses, such as metabolic stress (33,34). Direct treatment of clusterin dramatically reduced DNMT1 expression in tumor cells and resulted in GAD1 up-regulation (Fig 4E, right, white boxes, p < 0.00001) and a decrease in DNMT1 (Fig 4E, right, gray boxes, p < 0.00005). To examine whether glia-derived clusterin is responsible for DNMT1 reduction in tumor cells, we conducted loss-of-function experiment

by knocking down clusterin in glia cells prior to co-culture. Knocking down glia clusterin mRNA expression (Fig 4F, left, p < 0.00001) led to a decrease in GAD1 mRNA (Fig 4F, right, white boxes, p < 0.005) and an increase in DNMT1 mRNA (Fig 4F, right, grey boxes, p < 0.005) in the tumor cells after 48 hour co-culture. To determine whether the brain-microenvironment-induced reduction of DNMT1 is required for increased GAD1, we overexpressed DNMT1 in tumor cells (Fig 4G, left, p < 0.0001) resulting in blocking glia-induced GAD1 up-regulation (Fig 4G, right, p < 0.0001), and proliferative advantage (Fig 4H, p < 0.0005). Lastly, we targeted DNMT1 in tumor cells using an esiRNA (Supplementary Fig 5F, left, p < 0.0001) resulting in increased GAD1 expression in tumor cells (Supplementary Fig S5F, right, p < 0.0001). As both DNA methylation and histone modification status could potentially influences GAD1 expression, we further explored mRNA expression levels of histone modification enzymes in primary tumor and brain metastases microarray datasets. Surprisingly, we observed a general down-regulation of a majority of these enzymes (Supplementary Fig S6A). Using pair primary and brain metastases *in vivo* tissue sample, we validated the down-regulation of histone deactylase 1 (HDAC1) mRNA brain metastasis tissues (Supplementary Fig S6B, p < 0.005). Due to the generally low expression of HDACs, treating tumor cells with HDAC inhibitors did not result in a convincing restoration of GAD1 mRNA expression *in vitro* and *in vivo* (Supplementary Fig S6C-D), suggesting the HDACs-mediated mechanism is unlikely to be the major contributor in GAD1 expression. Taken together, comprehensive epigenetic analysis suggests brain-microenvironment-secreted clusterin down-regulates DNMT1 in metastatic tumor cells, which subsequently leads to GAD1 upregulation.

GAD1 Mediates a Dynamic Glutamine Metabolic Flux

Considering the role of GAD1 in regulating glutamine-GABA metabolism, we hypothesized that up-regulation of GAD1 drives a metabolic shift towards glutamine-mediated metabolism. To visualize cellular metabolic events dynamically, we transfected MBA-MD-231 with a biosensor for real-time sensing of cytosolic $NADH:NAD^+$ (Peredox)(25). Increased GFP/RFP ratio (Green/Red ratio) as reported by time-lapse imaging of Peredox indicates NADH accumulation in the cytosol and a more oxidative cellular status(35). We co-cultured tumor cells transfected with Peredox with either CAFs or primary glia cells under the precise control of media circulation, which allows us to alter extracellular glutamine concentrations and monitor intracellular $NADH/NAD^+$ in real-time (Fig 5A). After an initial starvation period with glucose-free and glutamine-free media for 15 minutes (T0 to T1), we introduced glutamine into the co-culture (Supplementary Fig 7A-B, T1). The glia co-cultured tumor cells responded dramatically to the glutamine, displaying a sharp decrease in green/red fluorescence ratio indicating increased consumption of NADH, while the CAF co-cultured tumor cells expressed a stable fluorescence signal, indicating no change in the NADH/NAD+ ratio (Supplementary Fig 7A-B, T1 to T2). Upon removing glutamine, all tumor cells, regardless of co-culture condition, showed an increase in green/red fluorescence ratio (Supplementary Fig 7A-B, T2 to T3). This data suggests that glia co-cultured tumor cells have a greater response to extracellular glutamine due to the brain stromal-cell-directed metabolic shift. When applying glucose containing media instead of glutamine-high media, we observed no increase in green/red fluorescence ratio (Supplementary Fig 7C, T1 to T2). This suggests that glia cells shift the tumor cells to

respond primarily to glutamine greater than glucose, a metabolite found in greater level in the brain parenchyma(36). To further characterize intracellular signaling in response to glutamine, we stained for phosphorylated AMPK (Thr172)(p-AMPK), a sensor of cellular energy homeostasis(37), at different time points during the glutamine starvation-replenish cycle. Under co-culture with CAFs, p-AMPK in tumor cells increases during the starvation period and remains unchanged during the subsequent high glutamine and starvation periods whereas the p-AMPK fluctuates moderately in the tumor cells co-cultured with glia (Supplementary Fig 8A-B). This result suggests that glia facilitates the ability of tumor cells to overcome metabolic stresses imposed by nutrient starvation.

To visualize the metabolic flux regulated by GAD1 expression, we co-cultured glia cells with tumor cells transfected with either GAD1 siRNA or a non-silencing control siRNA (Supplementary Fig S8C, left, p < 0.01). We observed an increase of the green/red ratio in all tumors cells during the initial starvation period (Fig 5B-C, T0 to T1). Once glutamine was introduced into the media, tumor cells transfected with siGAD1 did not respond to glutamine (Fig 5B, T1 to T2). Real-time imaging revealed a continuous increase of the green/red ratio in siGAD1 cells, despite co-culture with glia cells (Fig 5C). However, in the control siRNA group, replenishing glutamine led to an immediate decrease of the green/red ratio (Fig 5B-C, T1 to T2). When glutamine was removed from the media, all of the tumor cells display an increased green/red ratio, suggesting a more oxidative cellular status (Fig 5C, T2 to T3). Furthermore, increased staining of p-AMPK in tumor cells co-cultured with primary glia cells in response to glutamine starvation (T0 to T1) suggested an increase in anabolic metabolic pathways (Fig 5D-E and Supplementary Fig 8C, right). Consistent with this cellular behavior, when glia-induced overexpression of GAD1 was inhibited with siGAD1, tumor cells failed to utilize glutamine replenishment (T1 to T2), indicated by sustained staining of p-AMPK (Fig 5E). Taken together, demonstrate that glia-induced GAD1 is the key cellular metabolism enzyme responsible for the dynamic glutamine utilization capability of tumor cells, following metabolic shifting at the brain metastatic microenvironment.

Repurposing Vigabatrin as an anti-Brain Metastatic Therapy

The reliance on brain microenvironment-dependent GAD1 upregulation to drive glutamine metabolism and cell proliferation represents a novel therapeutic opportunity for brain metastasis treatment. Modulation of GAD1-mediated GABA metabolism has been clinically exploited previously as an anti-seizure therapy(38,39). One such drug, vigabatrin, targets GABA metabolism by inhibiting GABA transaminase (GABA-T), an enzyme directly downstream of GAD1. Vigabatrin thus functions to block GABA flux into the TCA cycle(40). Due to the essential role of GAD1-mediated GABA signaling in metastatic outgrowth, we hypothesize that vigabatrin could be repurposed to block tumor cells utilization of GABA as a metabolite, thereby decreasing metastatic outgrowth. Examination of GABA-T expression revealed an increase in both brain metastatic tumor samples (Fig 6A, left, p < 0.05) and tumor cells co-cultured with glia cells (Fig 6A, right, p < 0.05), which is likely to be a result of downstream positive feedback in response to up-regulated GAD1-GABA signaling. Knocking down GABA-T genetically (Fig 6B, p < 0.005) did not alter the GAD1 expression (Supplementary Fig S9A), but decreased glia-induced tumor cell

proliferation in both the MDA-MB-231 (Fig 6C, left, $p < 0.05$) and A375SM cell lines (Fig 6C, right, $p < 0.00005$), suggesting GABA-T is a downstream singling node responsible for GAD1's tumor promoting function. Consistently, targeting GABA-T pharmacologically with vigabatrin resulted in a dose-dependent reduction in tumor cell proliferation under glia co-culture (Fig 6D, $p < 0.05$), without significant impacts on the migratory potential of the tumor cells (Supplementary Fig S9B). Collectively, this data suggests that targeting GABA-T is a potentially viable brain metastasis therapy, which could block the proliferation potential of tumor cells in the brain microenvironment.

To explore the possibility of targeting the GAD1 metabolic pathway as anti-brain metastasis therapy *in vivo*, we induced shRNA expression after metastatic extravasation of tumor cells (seven days after intracarotid injection) (Supplementary Fig S9C). We observed a significant decrease in metastases with shGAD1 (GFP) compared to control shRNA cells (RFP) in both the A375SM (Fig 7A, $p < 0.05$) and MDA-MB-231 models (Fig 7B, $p < 0.00001$). This data suggests ablation of brain microenvironment-induced metabolic shifting to GAD1-GABA signaling is critical for successful brain metastatic outgrowth. Since we have demonstrated targeting GABA-T effectively suppressed tumor cell proliferation, we treated metastasis-bearing mice with either 4 mg/kg (clinically recommended dosage for anti-seizure treatment) or 7 mg/kg vigabatrin daily intraperitoneally. As expected, inhibiting GABA-T led to an evident accumulation of GABA in tumor cells in vitro (Supplementary Fig S9D, $p = 0.0218$). After a 7-day course of 4 mg/kg daily vigabatrin, the metastatic burden is dramatically decreased compared with vehicle-treated mice (Fig 7C). There were no detectable morphological differences in residual brain metastases (Fig 7D, left, H&E staining). We observed a dose-dependent decrease in the number of metastases (Fig 7D, right, $p < 0.01$), which is associated with a decrease in Ki-67$^+$ tumor cells (Fig 7E, $p < 0.05$). Together, these data suggest that blocking GABA flux into the TCA cycle, either through genetic depletion of GAD1 or pharmacological treatment with vigabatrin, significantly suppressed aggressive metastatic outgrowth in the brain.

Discussion

One of the emerging hallmarks of cancer is deregulated metabolism(41). Yet, the dynamic nature of metabolic reprogramming in response to metastatic microenvironments, such as the brain, has not been fully characterized. During the metastatic process, highly metastatic "seeds" from the primary tumor microenvironment experience a series of metabolic stresses and ultimately settle in an exotic metastatic microenvironment: the brain, an organ which maintains a unique metabolism equilibrium(7,11). Our study illustrates the striking metabolic plasticity of metastatic tumor cells. In order to take the greatest advantage of available metabolites, metastatic tumor cells, regardless of their primary tumor-of-origin, metabolically adapt to the brain microenvironment by engaging the GAD1-GABA synthesis pathway to facilitate metastatic outgrowth (Fig 7F). In accordance with the previous observation of upregulated GABA-receptors in brain metastatic tumors derived from HER2-positive breast cancer patients(16), our study significantly expands the relevance of this finding by revealing a mechanism of epigenetic up-regulation of the key GABA synthesis enzyme GAD1 in multiple tumor types which drives an increased intracellular GABA

metabolism. Our study also highlighted a clinically targetable mechanism for brain metastasis treatment (Fig 7F).

The data from this study shed light on the emerging concept of metastatic co-option. Co-option is essential to many biological ecosystems including disease conditions(42). Conceivably, metastasis, as a well-known multistep, tissue context-dependent biological process, requires a series of co-options to facilitate ultimate metastasis success. Indeed, during early metastatic colonization, blood vessel co-option has been observed and is believed to be essential for metastasis outgrowth(43). In our study, we demonstrated an indispensable form of metabolic co-option, in which metastatic tumor cells mimic astrocyte-neuron cooperation, by adopting a similar metabolic phenotype. Cooperation between astrocytes and neurons enables metabolic compartmentalization and precise metabolite regulation between astrocytes and neurons(7,11). In the normal brain tissue, glutamine metabolism primarily occurs in the astrocytes yet GABA synthesis occurs predominately in GABAergic neurons(7,11). Reminiscent of neurological disorders(29), metastatic tumor cells exhibit methylation-dependent up-regulation of GAD1, which is a marker of GABAergic neurons(44) and decrease of other glutamine catabolic process (Fig 2A-C and Supplemental Fig 2B-C). The altered metabolic phenotype, characterized by neuronal-like expression of the GAD1-GABA pathway, favors GABA synthesis in tumor cells and subsequently enables tumor cells to thrive in the glutamine-rich brain metastatic microenvironment. Due to the overarching role of DNMT1 in regulation of DNA methylation, it is reasonable to envision that a collective transcriptome shifting of a number of DNMT1-regulated genes orchestrates the highly dynamic brain metastasis process. Further study would be necessary to functionally reveal and validate other significant contributors in the brain metastasis context.

Furthermore, our data lays the groundwork for clinically translatable-targeted therapies for patients suffering with brain metastases. Currently, brain metastasis patients have limited treatment options, mainly surgery or radiotherapy(45). One of the major obstacles in developing therapies for brain metastasis is the presence of the blood brain barrier (BBB). The BBB acts as the barrier to prevent molecules from the vascular system from reaching the brain parenchyma(46). Most chemotherapeutic drugs fail to cross the BBB, making the brain a sanctuary organ for cancer cells(47). Fortunately, in developing treatments for mental disorders, there is a repertoire of clinical neurological drugs that have been proven to cross the BBB. Mechanistically, our data illustrates that brain metastatic tumor cells up-regulate a shared common signaling node, GAD1-GABA, with clinical seizures, which has been successfully targeted by the neurological drug, vigabatrin(39). Vigabatrin acts a suicide inhibitor of the enzyme directly downstream of GAD1, GABA transaminase (GABA-T), leading to an accumulation of GABA. For patients suffering from epilepsy, the increased pool of GABA results in a decrease in epileptic seizures(40). At the same time, inhibiting GABA-T also prevents GABA flux into the TCA cycle in tumor cells, suggesting that repurposing this neurological drug for brain metastasis may inhibit tumor GABA metabolism. One previous study suggested that treatment of HER2-positive breast cancer cells with vigabatrin decreases proliferation *in vitro*(16). Our study further demonstrated vigabatrin as a highly promising brain metastasis therapy using an *in vivo* model of brain metastases (Fig 7C-E). Expanding the applicability of these findings for additional brain

metastases that arise from other cancer is of interest for further study. Extravagated tumor cells lose their metastatic outgrowth capability in brain when vigabatrin is used to block GABA flux, decreasing both metastasis number and proliferation index (Fig 7C-E). It is important to note that brain tumor patients frequently experience seizures due to the deprivation of inhibitory neurotransmitter GABA around the tumor site(48). This suggests that in addition to treating brain metastases, vigabatrin might bring an additional benefit of stabilizing tumor-induced seizures, which is of interest for future pre-clinical and clinical study. Collectively, our study provides critical preclinical mechanistic evidence to support future clinical repurposing of FDA-approved GABA pathway targeting vigabatrin for brain metastatic patients.

In summary, our data demonstrates brain metastatic tumor cells adapt to the brain microenvironment by increasing GABA synthesis mediated by methylation-dependent up-regulation of GAD1. The dependence of brain metastatic cells on GAD1 and GABA reveals novel mechanistic insights into brain metastasis progression and, more importantly, provides intriguing rationale for repurposing neurological drugs as novel brain metastasis treatments.

Supplementary Material

Refer to Web version on PubMed Central for supplementary material.

Acknowledgments

References

1. Fidler IJ. The pathogenesis of cancer metastasis: the "seed and soil" hypothesis revisited. Nat Rev Cancer. 2003; 3:453–8. [PubMed: 12778135]

2. Hanahan D, Weinberg RA. Hallmarks of Cancer: The Next Generation. Cell. 2011; 144:646–74. [PubMed: 21376230]

3. Massagué J, Obenauf AC. Metastatic colonization by circulating tumour cells. Nature. 2016; 529:298–306. [PubMed: 26791720]

4. Nieman KM, Kenny HA, Penicka CV, Ladanyi A, Buell-Gutbrod R, Zillhardt MR, et al. Adipocytes promote ovarian cancer metastasis and provide energy for rapid tumor growth. Nat Med. 2011; 17:1498–503. [PubMed: 22037646]

5. Loo JM, Scherl A, Nguyen A, Man FY, Weinberg E, Zeng Z, et al. Extracellular Metabolic Energetics Can Promote Cancer Progression. Cell. 2015; 160:393–406. [PubMed: 25601461]

6. Chen EI, Hewel J, Krueger JS, Tiraby C, Weber MR, Kralli A, et al. Adaptation of Energy Metabolism in Breast Cancer Brain Metastases. Cancer Res. 2007; 67:1472–86. [PubMed: 17308085]

7. Cahoy JD, Emery B, Kaushal A, Foo LC, Zamanian JL, Christopherson KS, et al. A Transcriptome Database for Astrocytes, Neurons, and Oligodendrocytes: A New Resource for Understanding Brain Development and Function. J Neurosci. 2008; 28:264–78. [PubMed: 18171944]

8. Chowdhury GMI, Patel AB, Mason GF, Rothman DL, Behar KL. Glutamatergic and GABAergic neurotransmitter cycling and energy metabolism in rat cerebral cortex during postnatal development. J Cereb Blood Flow Metab. 2007; 27:1895–907. [PubMed: 17440492]

9. Çakır T, Alsan S, Sayba ılı H, Akın A, Ülgen KÖ. Reconstruction and flux analysis of coupling between metabolic pathways of astrocytes and neurons: application to cerebral hypoxia. Theor Biol Med Model. 2007; 4:48. [PubMed: 18070347]

10. Shank RP, Campbell GLM. α-Ketoglutarate and Malate Uptake and Metabolism by Synaptosomes: Further Evidence for an Astrocyte-to-Neuron Metabolic Shuttle. J Neurochem. 1984; 42:1153–61. [PubMed: 6699641]

11. Bélanger M, Allaman I, Magistretti PJ. Brain Energy Metabolism: Focus on Astrocyte-Neuron Metabolic Cooperation. Cell Metab. 2011; 14:724–38. [PubMed: 22152301]

12. Magistretti PJ. Role of glutamate in neuron-glia metabolic coupling. Am J Clin Nutr. 2009; 90:875S–880S. [PubMed: 19571222]

13. Magistretti PJ, Pellerin L. Astrocytes Couple Synaptic Activity to Glucose Utilization in the Brain. Physiology. 1999; 14:177–82.

14. Zhang L, Zhang S, Yao J, Lowery FJ, Zhang Q, Huang WC, et al. Microenvironment-induced PTEN loss by exosomal microRNA primes brain metastasis outgrowth. Nature. 2015

15. Chen Q, Boire A, Jin X, Valiente M, Er EE, Lopez-Soto A, et al. Carcinoma–astrocyte gap junctions promote brain metastasis by cGAMP transfer. Nature. 2016; 533:493–8. [PubMed: 27225120]

16. Neman J, Termini J, Wilczynski S, Vaidehi N, Choy C, Kowolik CM, et al. Human breast cancer metastases to the brain display GABAergic properties in the neural niche. Proc Natl Acad Sci. 2014 201322098.

17. Park ES, Kim SJ, Kim SW, Yoon SL, Leem SH, Kim SB, et al. Cross-species hybridization of microarrays for studying tumor transcriptome of brain metastasis. Proc Natl Acad Sci. 2011; 108:17456–61. [PubMed: 21987811]

18. Mecha M, Inigo PM, Mestre L, Hernangomez M, Borrell J, Guaza C. An easy and fast way to obtain a high number of glia cells from rat cerebral tissue: A beginners approach. Protoc Exch. 2011

19. Park ES, Kim SJ, Kim SW, Yoon SL, Leem SH, Kim SB, et al. Cross-species hybridization of microarrays for studying tumor transcriptome of brain metastasis. Proc Natl Acad Sci. 2011; 108:17456–61. [PubMed: 21987811]

20. Subramanian A, Tamayo P, Mootha VK, Mukherjee S, Ebert BL, Gillette MA, et al. Gene set enrichment analysis: A knowledge-based approach for interpreting genome-wide expression profiles. Proc Natl Acad Sci U S A. 2005; 102:15545–50. [PubMed: 16199517]

21. Reich M, Liefeld T, Gould J, Lerner J, Tamayo P, Mesirov JP. GenePattern 2.0. Nat Genet. 2006; 38:500–1. [PubMed: 16642009]

22. Xia J, Benner MJ, Hancock REW. NetworkAnalyst - integrative approaches for protein–protein interaction network analysis and visual exploration. Nucleic Acids Res. 2014; 42:W167–74. [PubMed: 24861621]

23. Xia J, Gill EE, Hancock REW. NetworkAnalyst for statistical, visual and network-based meta-analysis of gene expression data. Nat Protoc. 2015; 10:823–44. [PubMed: 25950236]

24. Li LC, Dahiya R. MethPrimer: designing primers for methylation PCRs. Bioinformatics. 2002; 18:1427–31. [PubMed: 12424112]

25. Hung YP, Albeck JG, Tantama M, Yellen G. Imaging Cytosolic NADH-NAD+ Redox State with a Genetically Encoded Fluorescent Biosensor. Cell Metab. 2011; 14:545–54. [PubMed: 21982714]

26. Chebib M, Johnston GAR. The "abc" of Gaba Receptors: A Brief Review. Clin Exp Pharmacol Physiol. 1999; 26:937–40. [PubMed: 10561820]

27. Pinal CS, Tobin AJ. Uniqueness and redundancy in GABA production. Perspect Dev Neurobiol. 1998; 5:109–18. [PubMed: 9777629]

28. Sotgia F, Galdo FD, Casimiro MC, Bonuccelli G, Mercier I, Whitaker-Menezes D, et al. Caveolin-1−/− Null Mammary Stromal Fibroblasts Share Characteristics with Human Breast Cancer-Associated Fibroblasts. Am J Pathol. 2009; 174:746–61. [PubMed: 19234134]

29. Dong E, Ruzicka WB, Grayson DR, Guidotti A. DNA-methyltransferase1 (DNMT1) binding to CpG rich GABAergic and BDNF promoters is increased in the brain of schizophrenia and bipolar disorder patients. Schizophr Res. 2015; 167:35–41. [PubMed: 25476119]

30. Consortium TEP. An integrated encyclopedia of DNA elements in the human genome. Nature. 2012; 489:57–74. [PubMed: 22955616]

31. Chen Y, Dong E, Grayson DR. Analysis of the GAD1 promoter: Trans-acting factors and DNA methylation converge on the 5′ untranslated region. Neuropharmacology. 2011; 60:1075–87. [PubMed: 20869372]

32. Jones PA. Functions of DNA methylation: islands, start sites, gene bodies and beyond. Nat Rev Genet. 2012; 13:484–92. [PubMed: 22641018]

33. Athanas KM, Mauney SL, Woo TUW. Increased extracellular clusterin in the prefrontal cortex in schizophrenia. Schizophr Res. 2015; 169:381–5. [PubMed: 26482819]

34. Pucci S, Mazzarelli P, Nucci C, Ricci F, Spagnoli LG. CLU "in and out": looking for a link. Adv Cancer Res. 2009; 105:93–113. [PubMed: 19879425]

35. Teodoro JS, Rolo AP, Palmeira CM. The NAD ratio redox paradox: why does too much reductive power cause oxidative stress? Toxicol Mech Methods. 2013; 235:297–302. 2013;23:297–302.

36. Yudkoff M, Nissim I, Daikhin Y, Lin ZP, Nelson D, Pleasure D, et al. Brain Glutamate Metabolism: Neuronal-Astroglia Relationships. Dev Neurosci. 1993; 15:343–50. [PubMed: 7805588]

37. Hardie DG. AMP-activated protein kinase—an energy sensor that regulates all aspects of cell function. Genes Dev. 2011; 25:1895–908. [PubMed: 21937710]

38. Sugino K, Hempel CM, Miller MN, Hattox AM, Shapiro P, Wu C, et al. Molecular taxonomy of major neuronal classes in the adult mouse forebrain. Nat Neurosci. 2006; 9:99–107. [PubMed: 16369481]

39. Grant SM, Heel RC. Vigabatrin. Drugs. 2012; 41:889–926.

40. Tolman JA, Faulkner MA. Vigabatrin: a comprehensive review of drug properties including clinical updates following recent FDA approval. Expert Opin Pharmacother. 2009; 10:3077–89. [PubMed: 19954276]

41. Pavlova NN, Thompson CB. The Emerging Hallmarks of Cancer Metabolism. Cell Metab. 2016; 23:27–47. [PubMed: 26771115]

42. True JR, Carroll SB. Gene Co-Option in Physiological and Morphological Evolution. Annu Rev Cell Dev Biol. 2002; 18:53–80. [PubMed: 12142278]

43. Yancopoulos GD, Davis S, Gale NW, Rudge JS, Wiegand SJ, Holash J. Vascular-specific growth factors and blood vessel formation. Nature. 2000; 407:242–8. [PubMed: 11001067]

44. Kodama T, Guerrero S, Shin M, Moghadam S, Faulstich M, Lac S du. Neuronal Classification and Marker Gene Identification via Single-Cell Expression Profiling of Brainstem Vestibular Neurons Subserving Cerebellar Learning. J Neurosci. 2012; 32:7819–31. [PubMed: 22674258]

45. Langer CJ, Mehta MP. Current Management of Brain Metastases, With a Focus on Systemic Options. J Clin Oncol. 2005; 23:6207–19. [PubMed: 16135488]

46. Abbott NJ, Rönnbäck L, Hansson E. Astrocyte–endothelial interactions at the blood–brain barrier. Nat Rev Neurosci. 2006; 7:41–53. [PubMed: 16371949]

47. Steeg PS. Targeting metastasis. Nat Rev Cancer. 2016; 16:201–18. [PubMed: 27009393]

48. Schaller B, Rüegg SJ. Brain Tumor and Seizures: Pathophysiology and Its Implications for Treatment Revisited. Epilepsia. 2003; 44:1223–32. [PubMed: 12919395]
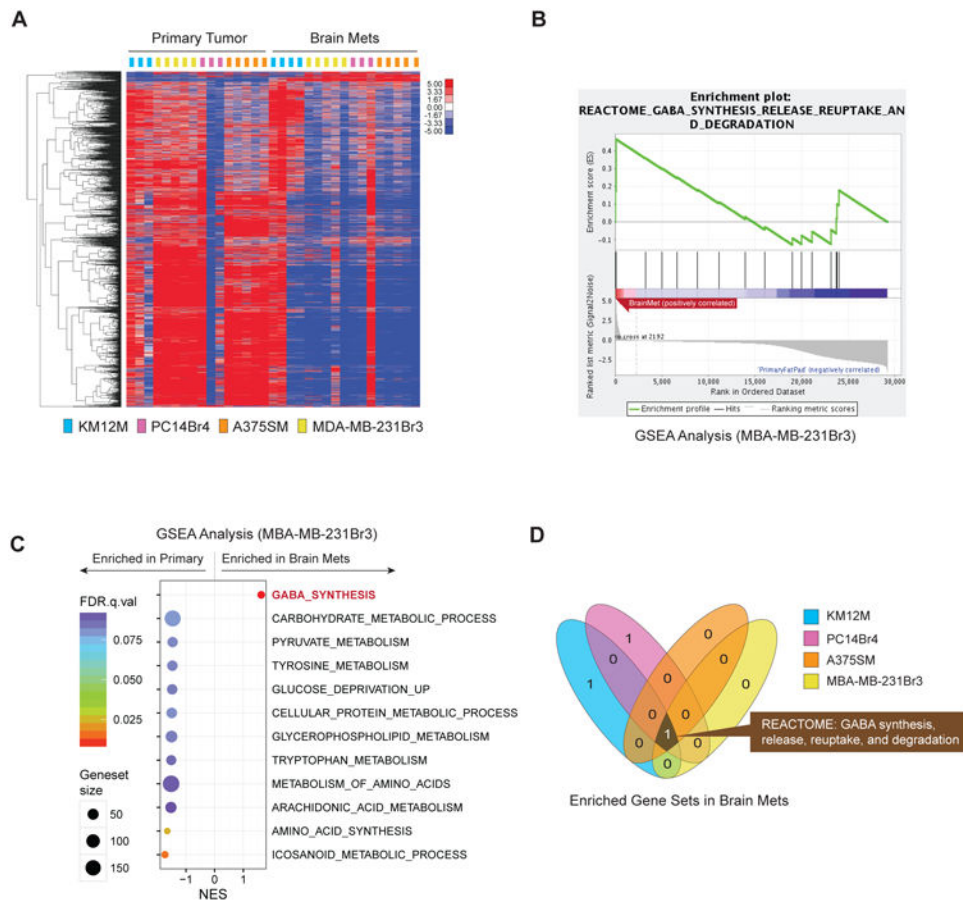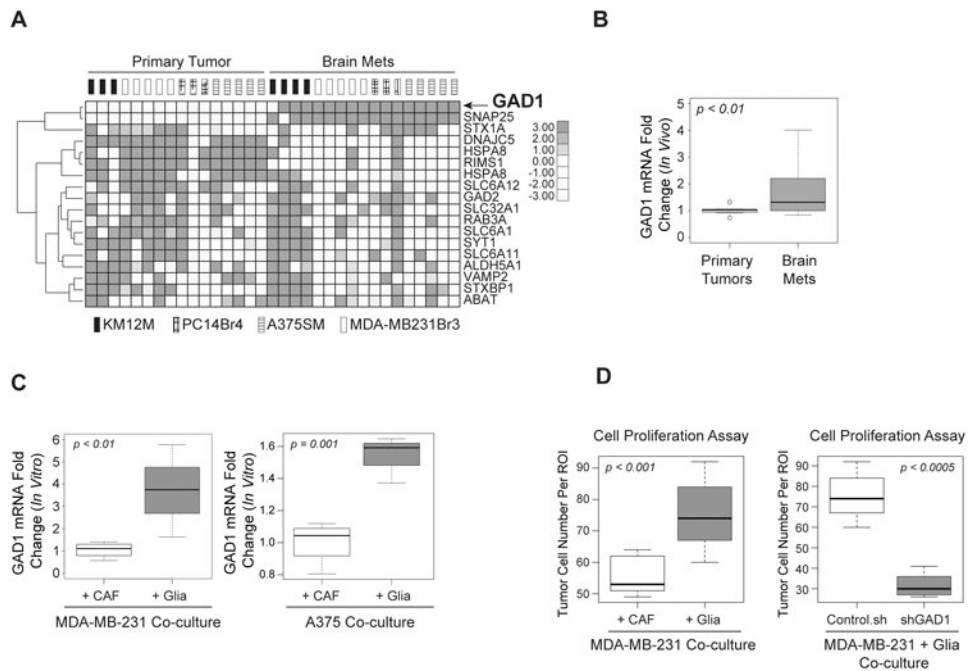
Figure 1.

Metastatic Microenvironment Induces Metabolic Transcriptome Shift. **A**, Heatmap of differentially expressed metabolic genes identified from bioinformatic analysis of GSE19184. **B**, GSEA result of gene sets enriched in either brain metastatic or primary tumor samples arising from MDA-MB-231Br3. **C**, Cleveland plot of top 10 gene sets enriched in either brain metastatic or primary tumor samples arising from MDA-MB-231Br3. **D**, Venn diagram of gene sets enriched in the brain metastatic samples arising from indicated cell lines.

Figure 2.
Brain Microenvironment Induces GAD1 Upregulation. **A**, Heat map of Reactome: GABA synthesis, release, reuptake, and degradation gene set from bioinformatic analysis of GSE19184. **B**, qRT-PCR validation of GAD1 mRNA expression using tissue samples of either primary or brain metastatic tumors derived from MDA-MB-231. **C**, qRT-PCR of GAD1 mRNA expression of tumor cells after 48 hours co-culture with either CAFs or glia cells. (left) MDA-MB-231; (right) A375SM **D**, (left) Cell proliferation assay of MDA-MB-231 after 48 hours of co-culture with CAF or primary glia cells. (right) Cell proliferation assay of MDA-MB-231 with or without knock-down of GAD1 by transfection with either control shRNA or GAD1-targeting shRNA prior to co-culture with primary glia cells for 48 hours with Dox-containing reduced media.
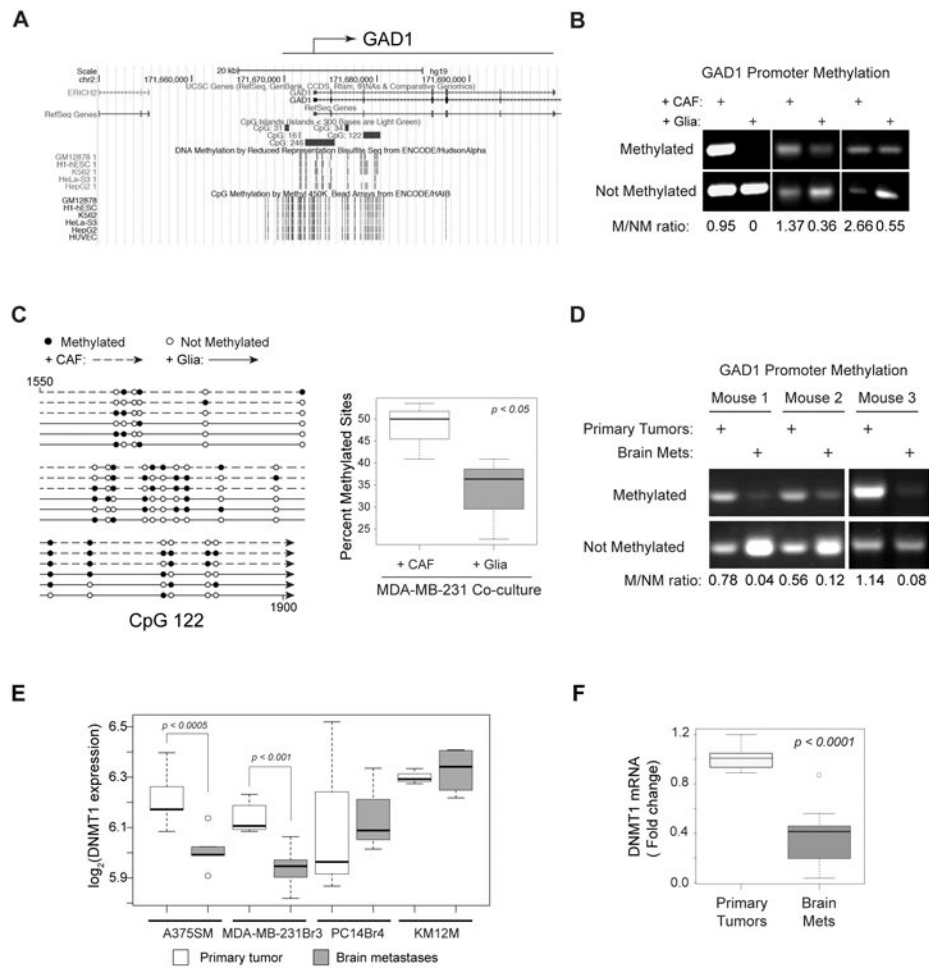
Figure 3.
Altered Tumor Cell GAD1 Promoter Methylation and DNMT1 Expression Induced by Brain
Microenvironment. **A**, UCSC Genome Browser plot of ENCODE data track of CpG Islands
located around the GAD1 promoter. **B**, Promoter methylation-specific PCR (MSP) assay
detecting methylation status in human GAD1 promoter region *in vitro*. **C**, (left) Bisulfite
sequencing of CpG island 122 located in human GAD1 promoter region, (right) Percentage
of Methylated CpG sites in sequenced region. **D**, MSP assay detecting methylation status in
the human GAD1 promoter region *in vivo*. **E**, Bioinformatics analysis of GSE19184
showing normalized DNMT1 probe intensity in primary tumors or brain metastases arising
from indicated cell lines. **F**, qRT-PCR of DNMT1 mRNA levels in primary tumors or brain
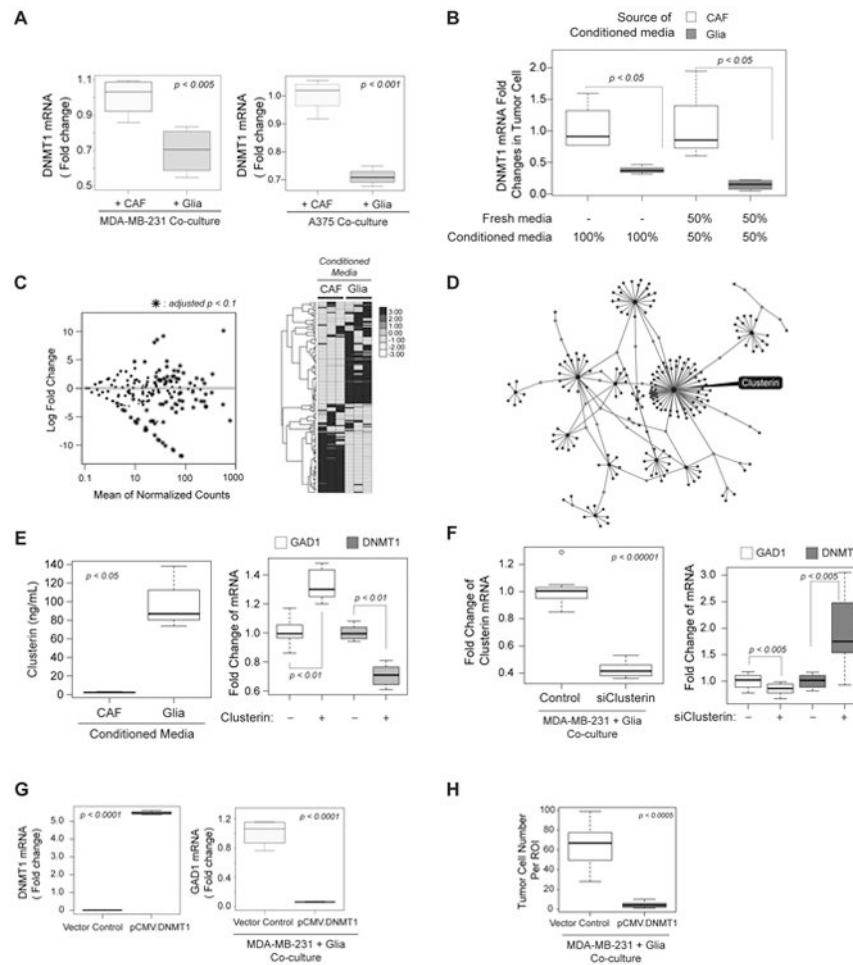metastases arising from MDA-MB231.

Figure 4.
Brain Microenvironment-Induced Down-Regulation of DNMT1 Reactivates GAD1
Expression. **A**, qRT-PCR of DNMT1 mRNA expression after 48 hours co-culture with either
CAF or glia cells. (left) MDA-MB-231; (right) A375SM. **B**, qRT-PCR of DNMT1 mRNA
expression of MDA-MB-231 cultured either with 100% conditioned media from either CAF
or glia cells or 50% mix of conditioned media and fresh media. **C**, Cytokine screen of glia
and CAF conditioned media. (left) MA plot of Log [mean expression of Glia/CAF] of 73
cytokines analyzed. *: differentially expressed cytokines (adjusted $p < 0.1$) (right) Heatmap
of differentially expressed cytokines. **D**, Network analysis of differentially expressed
cytokines. **E**, Impact of extracellular clusterin on DNMT1 and GAD1 expression. (left)
Cytokine expression profile of clusterin in conditioned media from CAFs or glia cells.
(right) qPCR of GAD1 and DNMT1 mRNA expression in MDA-MB-231 cells treated with
control or 200 ng of clusterin. **F**, qRT-PCR of GAD1 and DNMT1 mRNA expression in
tumor cells genetic knockdown of glia derived-clusterin. (left) qRT-PCR of clusterin mRNA
expression in glia cells. (right) qRT-PCR of GAD1 and DNMT1 mRNA expression in MDA-
MB-231 cells co-cultured with control glia or siClusterin glia cells. **G**, qRT-PCR of mRNA
levels in tumor cells after 48 hours co-culture with primary glia cells. Prior to co-culture,
tumor cells were transfected with either vector control or DNMT1 over expression plasmid

for 24 hours. (left) DNMT1 mRNA expression; (right) GAD1 mRNA expression under glia co-culture. **H,** Proliferation of MDA-MB-231 cells after DNMT1 overexpression and co-culture with glia cells for 48 hours.
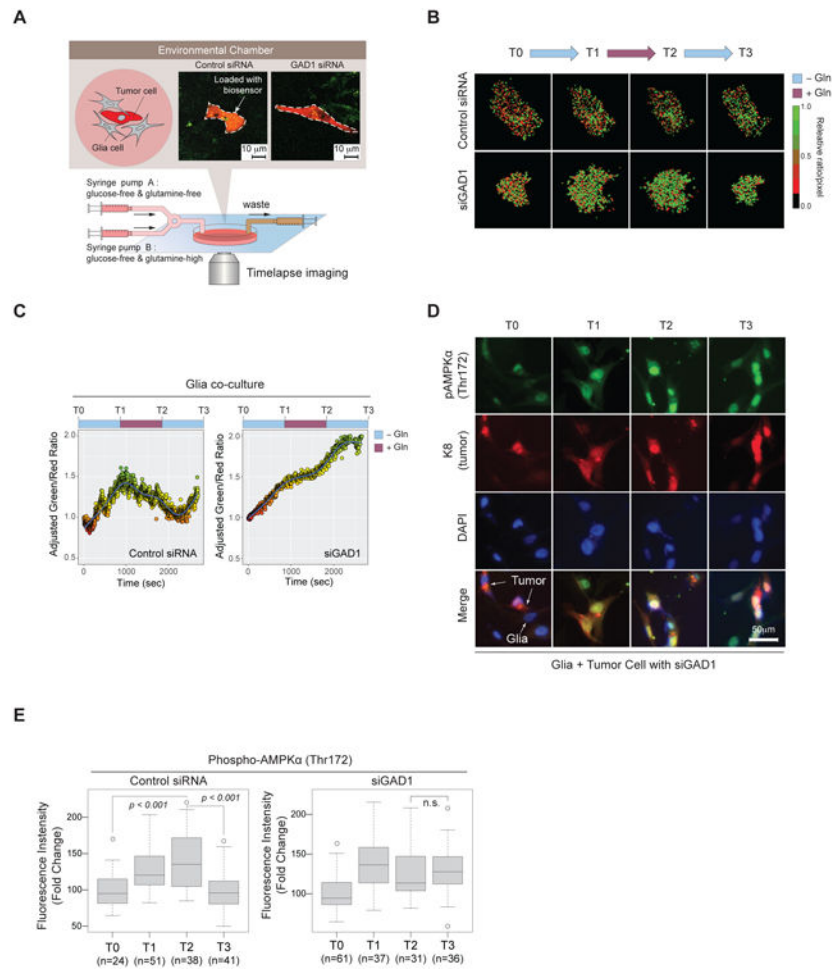
Figure 5.
GAD1 Mediates Dynamic Tumor Glutamine Metabolic Flux. **A**, Schematic of experimental setup. **B**, Heat maps of time course of changes in fluorescence ratio of Peredox biosensor throughout indicated time points. Prior to biosensor study, MDA-MB-231 were transfected with either control or GAD1 targeting siRNA for 24 hours; then co-cultured with glia cells for another 48 hours. T0: 48 hours co-culture in reduced media; T1: 15 minutes of incubation in glucose-free and glutamine-free media; T2: 15 minutes of incubation in glucose-free and 2 mM glutamine media. T3: 15 minutes of incubation in glucose-free and glutamine-free media. **C**, Time course measurements of green/red fluorescence ratio of Peredox biosensor in MDA-MB-231. Tumor cells were transfected, co-cultured and treated as in **B**. **D**, Representative images of immunofluorescence staining of tumor cell's phosphorylated AMPK at Thr172 (pAMPK) and tumor specific marker cytokeratin 8 (K8) at indicated time point after 48 hours co-culture with glia cells following transfection with GAD1 targeting siRNA. Time-course experiments (T0-T3) are conducted as **B**. **E**, Quantification of pAMPK fluorescence intensity in tumor cells from images in **D**.
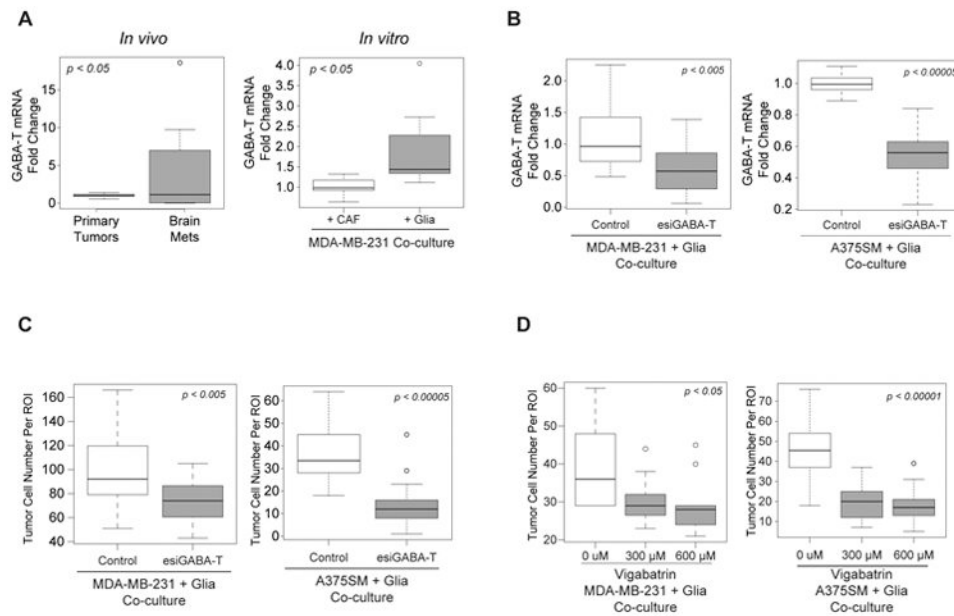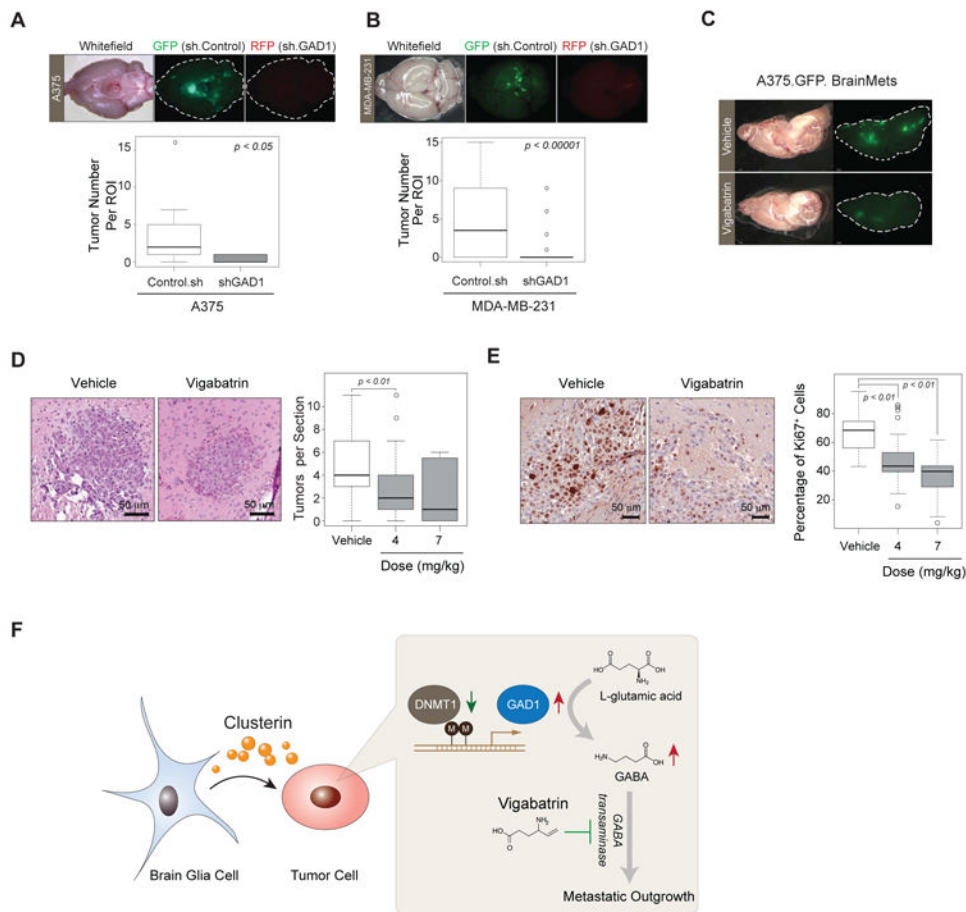
Figure 6.
Suppression of metastatic tumor cell proliferation *in vitro* by targeting GABA-T. **A**, qPCR of GABA-T mRNA expression. (left) primary tumor or brain metastatic samples arising from MDA-MB-231 cell line, (right) MDA-MB-231 cells co-cultured with either CAF or glia cells for 48 hours in reduced media. **B**, qPCR of GABA-T after tumors are transfected with esiRNA targeting GABA-T or control and then co-cultured with glia cells for 48 hours. (left) MDA-MB-231 cells; (right) A375SM cells. **C**, Proliferation of tumor cells after transfection with esiRNA targeting GABA-T or control and then co-culture with glia cells for 48 hours. (left) MDA-MB-231 cells; (right) A375SM cells. **D**, Proliferation of tumor cells after co-culture with glia cells and treatment of Vigabatrin, either control, 300 μM, or 600 μM. (left) MDA-MB-231 cells; (right) A375SM cells.

Figure 7.
GAD1-Mediated Glutamine Metabolism Enables Brain Metastatic Outgrowth. **A**, (top) Representative images of A375SM brain metastatic tumors arising from 1:1 mix of tumor cells expressing either control (labeled with GFP) or GAD1 targeted shRNA (labeled with RFP), (bottom) Quantification of metastatic incidence. **B**, (top) Representative images of MDA-MB-231 brain metastatic tumors with/without GAD1 knockdown, (bottom) Quantification of metastatic incidence. **C**, Representative images of brain metastatic tumors arising from arising from A375SM cell after treated with vehicle control or vigabatrin (4 mg/kg) for seven days beginning at seven days post injection. **D**, Reduction of metastatic tumor lesions by vigabatrin. (left) representative images of haemoxyolin and eosin staining of metastatic tumors treated with either control or vigabatrin (4 mg/kg); (right) Quantification of stained tumors per section. **E**, Ki-67 immunohistochemistry staining of tumors arising in mice treated with either vehicle control or vigabatrin (4 mg/kg). (left) Representative images of Ki-67 staining; (right) Quantification of ki-67 positive tumor cells per region of interest. **F**, Proposed model of brain microenvironment-induced tumor cell metabolic shifting via clusterin-mediated epigenetic upregulation of GAD1, which contributes to brain metastatic outgrowth.